Vol. 89: 43–53, 2023
https://doi.org/10.3354/ame01996

AQUATIC MICROBIAL ECOLOGY
Aquat Microb Ecol

Published March 30

Choice of methodology and surrogate prey are decisive for the quality of protistan bacterivory rate estimates

Javier Florenza[1,*], Stefan Bertilsson[1,2]

[1]Department of Ecology and Genetics, Uppsala University, 75236 Uppsala, Sweden
[2]Department of Aquatic Sciences and Assessment, Swedish University of Agricultural Sciences, 75651 Uppsala, Sweden

ABSTRACT: Microeukaryote predation on bacteria is a fundamental phenomenon to understand energy and nutrient dynamics at the base of the aquatic food web. To date, the most prevalent way to estimate grazing rates is by using epifluorescence microscopy to enumerate ingestion events of fluorescently labelled tracers (FLTs) after short-term incubation experiments. However, this approach can be sensitive to the type of FLT, requires skillful preparation of the samples and is limited to small sample sizes. We tested the susceptibility of rate estimates to the choice of prey and made a side-by-side comparison between microscopy and flow cytometry when recording ingestion by a bacterivorous flagellate. Short-term uptake experiments were established using 5 types of FLTs differing in quality (living, dead or inert) and size (large or small), with *Ochromonas triangulata* as a model flagellate. The experiments showed that (1) each of the different prey types yielded different clearing rates, ranging from 0.5 to 3.6 nl cell^{-1} h^{-1}, with the largest differences (3-fold or higher) between small prey (lower rates) and large prey (higher rates); (2) the cytometry estimate differed significantly from the microscopy estimate in 3 out of 4 experimental configurations; and (3) the precision of the cytometric analysis was greater, with >3-fold higher uncertainty associated with microscopy counting. Our results validate that flow cytometry provides a more precise bacterivory estimate, and that the choice of FLT influences the grazing rate estimate to a high extent regardless of the analytical method used.

KEY WORDS: Bacterivory rates · Fluorescently labelled tracers · FLB · Flow cytometry · *Ochromonas triangulata*

1. INTRODUCTION

Grazing of aquatic bacteria by phagotrophic protists occurs at the base of the aquatic food web, and is thus a fundamental process underpinning the dynamics of aquatic ecosystems. The rate and selectivity at which protists graze on bacteria are key factors for our understanding of, for instance, bacterial community composition (Šimek et al. 2002, 2014) or carbon and nutrient transfer through the microbial loop (Azam et al. 1983, Chrzanowski & Foster 2014, Grujčić et al. 2015) and are expected to fluctuate over time to a high degree, with pronounced dynamics over hourly (Pålsson & Granéli 2003) to seasonal timescales (Sanders et al. 1989, Domaizon et al. 2003, Princiotta & Sanders 2017). Therefore, accurate estimates of bacterivory rates are instrumental to reliably interpret the status and function of a given aquatic system and its community dynamics.

Typically, bacterivory by phagotrophic protists is measured by the addition of fluorescently labelled tracers (FLTs) to a sample. Grazing rates are then estimated by using epifluorescence microscopy to evaluate tracer uptake by protists over a short timespan or tracer disappearance from the sample over longer incubations (Caron 2001). FLT short-term uptake experiments are widely employed to support ecological claims, using either synthetic microspheres (e.g. Bird

*Corresponding author: xavi.florenza@ebc.uu.se

© The authors 2023. Open Access under Creative Commons by Attribution Licence. Use, distribution and reproduction are unrestricted. Authors and original publication must be credited.

Publisher: Inter-Research · www.int-res.com

& Kalff 1987, Domaizon et al. 2003, Princiotta & Sanders 2017) or fluorescently labelled bacteria (FLB; e.g. Arenovski et al. 1995, Massana et al. 2009, Wilken et al. 2018) as experimental prey surrogates. However, concerns associated with this approach have been articulated, including high statistical uncertainty associated with necessarily small (on the order of ~10^2 cells) sample sizes examined (Cleven & Weisse 2001), alterations introduced by fixation and slide preparation (Caron 2001), significant variation in grazing estimates associated with prey quality (Fu et al. 2003) or generic assumptions on grazing behavior attributed to all potentially feeding individuals in a sample (Cleven & Weisse 2001, Anderson et al. 2017).

Flow cytometry has the potential to overcome some of these issues, enabling the analysis of living samples and the screening of >10-fold larger sample sizes, thus providing a means to obtain more precise and statistically robust estimates. Solutions to estimate grazing rates from flow cytometry measurements have already been proposed, either based on monitoring prey disappearance (Vazquez-Dominguez et al. 1999, Fu et al. 2003) or targeting ingestion events by the predator (Keller et al. 1994, Bratvold et al. 2000, Costa et al. 2022). Of these studies, only Costa et al. (2022) attempted to compare flow cytometry against epifluorescence microscopy on the same study objects.

In the present study, flow cytometry is compared to epifluorescence microscopy for estimating bacterivory rates by the mixotrophic flagellate *Ochromonas triangulata*. This comparison is based on short-term FLT uptake experiments (i.e. focusing on FLT ingestion by the predator) carried out using 5 different FLT types as prey under otherwise identical experimental conditions. The FLTs under scrutiny differed in quality (microspheres, FLB and living bacteria carrying a fluorescent marker gene) and size (large and small). This combination of 2 observational methodologies with 5 different tracers allowed us to robustly contrast the performance of both techniques while providing further insights into the impact of prey size and quality on final grazing estimates.

2. MATERIALS AND METHODS

2.1. Strains and culture conditions

Clonal, unialgal, non-axenic stock cultures of *Ochromonas triangulata* strain RCC21 (obtained from the Roscoff Culture Collection) were grown in batch cultures of filter-sterilized K/2 medium (Keller et al. 1987, adjusted by I. Probert and further modified by substituting natural seawater for artificial seawater prepared according to Berges et al. 2001). The cultures were maintained at 18°C under a 12 h light: 12 h dark photoperiod (120 µmol m^{-2} s^{-1} photon flux measured with a QSL-100 spherical sensor; Biospherical Instruments) by transferring a 2 ml inoculum of each batch into 18 ml of fresh medium approximately every 3 wk. To ensure acclimation of the strain to the experimental conditions and homogeneous growth rates across replicates, a clone of *O. triangulata* was transferred into semicontinuous batch culture and kept for 14 generations at >0.8 doublings d^{-1} prior to the start of the experiment.

Wild-type *Escherichia coli* cells were grown from a glycerol-frozen stock by streaking an inoculum onto LB agar plates and incubating for 24 h at 37°C, after which a single clonal colony was resuspended in 3 ml of LB broth and left at 37°C under mild agitation. The culture was maintained in an actively growing state by subsequent duplicated transfers of 100 µl into 3 ml of fresh medium every 24 h until 5 ml of daily refreshed *E. coli* stock was transferred to 120 ml of fresh LB and grown at 37°C under constant agitation for 16 h prior to cell harvest for FLB preparation.

A liquid stock culture of *Limnohabitans* sp. strain Rim47 (Kasalický et al. 2013) was kept under constant agitation in 30 ml of NSY-IBM medium (Hahn et al. 2004) at 18°C and a 12 h light:12 h dark photoperiod for 21 d, at which point 25 ml of living stock was transferred into 125 ml of fresh medium and grown under the same conditions for 72 h prior to cell harvest for FLB preparation.

E. coli TOP10 cells bearing the plasmid pQE30-tGFP were grown from a glycerol-frozen stock on LB-carbenicillin (50 mg l^{-1}) plates for 24 h at 30°C, after which a single clonal colony was resuspended in 3 ml of LB-carbenicillin (1 mg l^{-1}) broth (LB-C) and grown at 30°C under mild agitation. After 16 h, 100 µl of this culture was transferred into 3 ml of LB-C broth and subsequently refreshed every 24 h until needed for the experiment.

2.2. FLB preparation

Bacterial cells permanently stained with fluorescein were prepared according to Sherr & Sherr (1993), both from *E. coli* and *Limnohabitans* sp. stocks. Briefly, cells were harvested by centrifugation of 20 ml fractions at 22 000 × *g* for 12 min. The supernatant was discarded and each pellet was resuspended in 1.5 ml of 0.2 mg ml^{-1} 5-(4,6-dichlorotriazin-2-yl)aminofluorescein (5-DTAF; Sigma Aldrich)

in freshly prepared 0.01 M phosphate-buffered saline (PBS) (pH adjusted to 9). Next, all fractions of the same strain were pooled together and incubated at 60°C for 2 h. After incubation, each pool was split again into 20 ml fractions, centrifuged at 22 000 × *g* for 12 min and washed with PBS. This washing step was repeated 3 more times, and the final pellets were resuspended in a saline (0.85% NaCl) 0.02 M $Na_2P_2O_7$ solution before being aliquoted and stored at −20°C until further use.

2.3. Prey surrogates

Five different fluorescent tracers were tested in this experiment (Table 1). Prey surrogates can be grouped into 2 size classes based on their volume (large or small) and 3 type classes based on their quality: inert (chemically inert polystyrene beads), dead (FLB derived from heat-killed cultured bacteria) and living (living cells expressing a fluorescent reporter). Inert types: Fluoresbrite® YG polystyrene microspheres with diameters of 0.51 µm (BDS-.5) and 0.98 µm (BDS-1) (catalog numbers 15 700 and 17 154, respectively; Polysciences) were diluted 1:1000 in 0.01 M PBS, vortexed and sonicated before incubations. FLB types: aliquots of FLB prepared from wild-type *E. coli* (FLB-E) or *Limnohabitans* sp. (FLB-R) stocks (see above for preparation protocol) were thawed, diluted 1:100 into 0.01 M PBS, vortexed and sonicated with three 3 s pulses of 5 W for satisfactory dispersion. Green fluorescent protein (GFP) type: a 100 µl aliquot of a 24 h old stock was resuspended in 3 ml LB-C and further grown at 30°C for 8 h, after which 100 µl was transferred to LB-C amended with 100 nM isopropyl β-D-thiogalactopyranoside (IGTP) final concentration to induce GFP expression and grown at 30°C overnight under constant agitation. GFP-expressing *E. coli* cells were harvested on the same day of the experiment by centrifuging the grown inoculum at 22 000 × *g* for 12 min and then washing in freshly prepared PBS. After 3 consecutive washing and centrifuging steps, the pellet was finally resuspended in 2 ml of PBS and kept at 4°C until use.

2.4. Experimental setup

A clonal, non-axenic culture of acclimated *O. triangulata* growing in semicontinuous culture (see Section 2.1) was inoculated into 12 flasks at a final culture volume of 40 ml. After 5 d of growth (0.98 doublings d^{-1}; growth curves for *O. triangulata* and its co-cultured bacterial population can be found in Fig. S1 in the Supplement at www.int-res.com/articles/suppl/a089p043_supp.pdf), all 12 cultures were pooled into a 500 ml sterile, clear plastic bottle immediately prior to the start of the FLT incubations. This was done to avoid undesired volume effects on *O. triangulata* growth while ensuring sufficient culture volume to complete the experiment. All FLT incubations were carried out in 75 ml clear plastic flasks starting with 30 ml of acclimated *O. triangulata* culture at 18°C and in the absence of light. Five min before the tracer addition, 5 µl of 1 mM LysoSensor™ (LS) Blue DND-167 (Invitrogen) was added to each culture. LS acts as a food vacuole stain (Carvalho & Granéli 2006) and was used here to determine the total feeding population of *O. triangulata* in the flow cytometer. Incubations with each prey surrogate were performed in triplicate, and all prey surrogates were inoculated at a final density of ~0.15 × 10^6 particles ml^{-1}, which corresponded to 8.5% of the total density of co-cultured bacteria in the flasks (~1.77 × 10^6 cells ml^{-1}; see Fig. S1B). Upon FLT addition, all flasks were sampled at time zero immediately after the addition of the tracer and were subsequently sampled at 4, 8, 12, 16, 20, 24, 32 and 40 min for cytometry and 8, 16, 24, 32 and 40 min for microscopy. For cytometry, 500 µl aliquots were immediately placed into a saline ice bath (−2 to −1.5°C) and

Table 1. Description and properties of the different types of fluorescently labelled tracers (FLTs) used in this study. CV: percent coefficient of variation

FLT code	Description	Length (µm)	Width (µm)	Volume ($µm^3$)	Size class	Quality class
BDS-.5	Polystyrene microspheres, 0.51 µm	–	–	0.070 (CV 9%)[a]	Small	Inert
BDS-1	Polystyrene microspheres, 0.98 µm	–	–	0.49 (CV 9%)	Large	Inert
FLB-R	Fluorescently labelled *Limnohabitans* sp. cells	0.78 (CV 25%)	0.43 (CV 22%)	0.097 (CV 55%)	Small	Dead
FLB-E	Fluorescently labelled *Escherichia coli* cells	2.06 (CV 27%)	0.72 (CV 15%)	0.76 (CV 41%)	Large	Dead
GFP	GFP-expressing *E. coli* TOP10 cells (plasmid pQE30-tGFP)	1.73 (CV 25%)	0.77 (CV 16%)	0.72 (CV 48%)	Large	Living

[a]Based on 3% CV in diameter values declared by the manufacturer

kept cold for analysis of unpreserved (live) cells as soon as possible (typically within 10 to 20 min). This procedure was based on previous tests where no further ingestion was observed after exposure to temperatures close to 0°C (Fig. S2). For microscopy, 2 ml aliquots were fixed with 2 ml freshly prepared, ice-cold 4% formaldehyde in PBS and kept frozen until slide preparation. For each replicate, both samples for cytometric and microscopic analyses were collected from the sample flask.

2.5. Flow cytometry

All cytometric measurements, including both cell and surrogate prey density measurements, were carried out on a CytoFLEX flow cytometer (Beckman Coulter) equipped with violet (405 nm) and blue (488 nm) lasers for excitation. Cell populations of *O. triangulata* were identified via side scatter signal (SSC) and chlorophyll autofluorescence was detected in the FL3 channel (EX 488, EM 690/50). Cell counts for total bacterial cells were based on separate samples stained with SYBR™ Green I nucleic acid stain (Invitrogen) detected in the FL1 channel (EX 488, EM 525/40). All prey surrogates bearing green constitutive fluorescence could be identified based on their signal in the FL1 channel.

For the experiment described in this study, the flow cytometer was set to a flow rate of 75 µl min^{-1} (yielding an average event rate of 44 s^{-1}), and acquisition time was set to 2 min for each sample. Counting gates were manually established, and thresholds to discriminate between prey-positive and prey-negative events were set as depicted in Fig. S3: the target *O. triangulata* population was identified via its signal in the SSC and FL3 channels, further refined based on the LS signal detected in the FL5 channel (EX 405, EM 450/45) and cell association to a tracer was evaluated based on FLT signal in the FL1 channel. The threshold between FLT-positive and FLT-negative cells was established with an FLT-free subsample of the same origin as the rest of the samples. Flow cytometry data are publicly available at FlowRepository, International Society for the Advancement of Cytometry, under experiment ID FR-FCM-Z64S.

2.6. Epifluorescence microscopy

Aliquots for microscopy were thawed overnight at 4°C prior to slide preparation; 4′,6-diamidino-2-phenylindole (DAPI; Sigma Aldrich) (2 µg ml^{-1} final concentration) was used as a counterstain by exposing the samples for at least 10 min. Fractions (2 ml) of fixed, stained samples were filtered through 3 µm pore size Nuclepore™ polycarbonate membrane filters (Cytiva), and the filters were mounted onto slides according to the filter–transfer–freeze technique (Hewes & Holm-Hansen 1983). Briefly, filters were deposited sample-side down onto a clean slide and placed onto a metal surface maintained at approximately −80°C. When frozen, the filter can be peeled away while the sample stays attached to solid moisture. A drop of glycerol-based, hard-setting mountant (ProLong™ Glass; Invitrogen) was placed on the slides upon filter removal and subsequently covered with a coverslip. Preparations were allowed to cure overnight at room temperature protected from light and stored at 4°C until observation.

All slides were examined at 1000× total magnification with a Nikon Eclipse E600 epifluorescence microscope equipped with a 100 W mercury short-arc lamp and the following filter sets: NQ-31 (EX 365/50, DM 405, EM 450/65; Omega Optical), UV-2A (EX 355/50, DM 400; EM 420 LP; Nikon) and B-2A (EX 470/40, DM 500, EM 520 LP; Nikon). Cells were identified based on DAPI (nucleus) fluorescence on either the NQ-31 or UV-2A filters, and the number of ingested fluorescent prey units, if any, was assessed using the B-2A filter (allowing simultaneous visualization of prey and chloroplasts). In doubtful cases (e.g. when prey could be adjacent but not necessarily ingested), pseudo phase contrast (phase contrast ring in the condenser with a regular epifluorescence objective) was used in conjunction with green fluorescence to evaluate the position of the prey based on cell contour. In the rare occurrences when the position of prey could not be resolved, the cell was not considered in the census. All preparations were scanned horizontally until a minimum of 5 full transects were examined and either (1) a cell count higher than 500 was reached or (2) a maximum of 10 full transects were examined. Example pictures of FLT ingestion (see Fig. 2) were obtained with an Olympus IX73 epifluorescence microscope equipped with the following filter sets: UV-to-blue (EX 365/10, DM 410, EM 440/40), blue-to-green (EX 482/25, DM 505, EM 530/40) and blue-to-red (EX 445/30, DM 510, EM 665 LP).

2.7. Clearance rate calculations

For the cytometry-based estimation, average number of tracer units per cell were calculated assuming that each event attributed as prey-positive repre-

sented one ingestion event in a one-to-one correspondence. Even though multiple ingestion events are easily traceable when using microspheres, this is not the case when using other FLTs. Therefore, we applied the simplest assumption described above to ensure comparability across FLT types. For the microscopy-based estimation, classes 0, 1, 2, 3 or 4 or more prey units were scored for each observed predator cell, and tracer units per cell were averaged across observations in each sample. Averages for the number of prey per cell over time were used in linear regressions to estimate tracer uptake rates (r) for each methodology and prey type, which in turn were used to estimate clearance rates (CRs) according to the following equation (Caron 2001):

$$\mathrm{CR} = r\,\frac{1}{D_{\mathrm{p}}} \qquad (1)$$

where D_{p} is the density of surrogate prey cells per unit volume in each incubation. See Table 2 for D_{p} values for all FLTs used in this experiment.

3. RESULTS

The 2 counting strategies outlined above resulted in sample sizes of 667 and 4847 cells replicate^{-1} (median values) from epifluorescence microscopy and flow cytometry, respectively (Fig. S4). In the former case, numbers refer to all individual cells assessed per replicate during observation, while in the latter case, they refer to all cells detected as actively feeding (i.e. LS-positive). For both methods, average estimates for the number of prey units per cell were calculated for each replicate based on these individual observations following the strategies described in Sections 2.5 & 2.6. No major difficulties associated with a particular prey type were experienced during microscopical examination of the samples, although the inert prey type (i.e. microspheres) posed less of a challenge when counting cases of multiple ingested particles by a single flagellate, given their homogeneous size and shape (Fig. 1A). Regarding flow cytometry, food vacuole staining re-

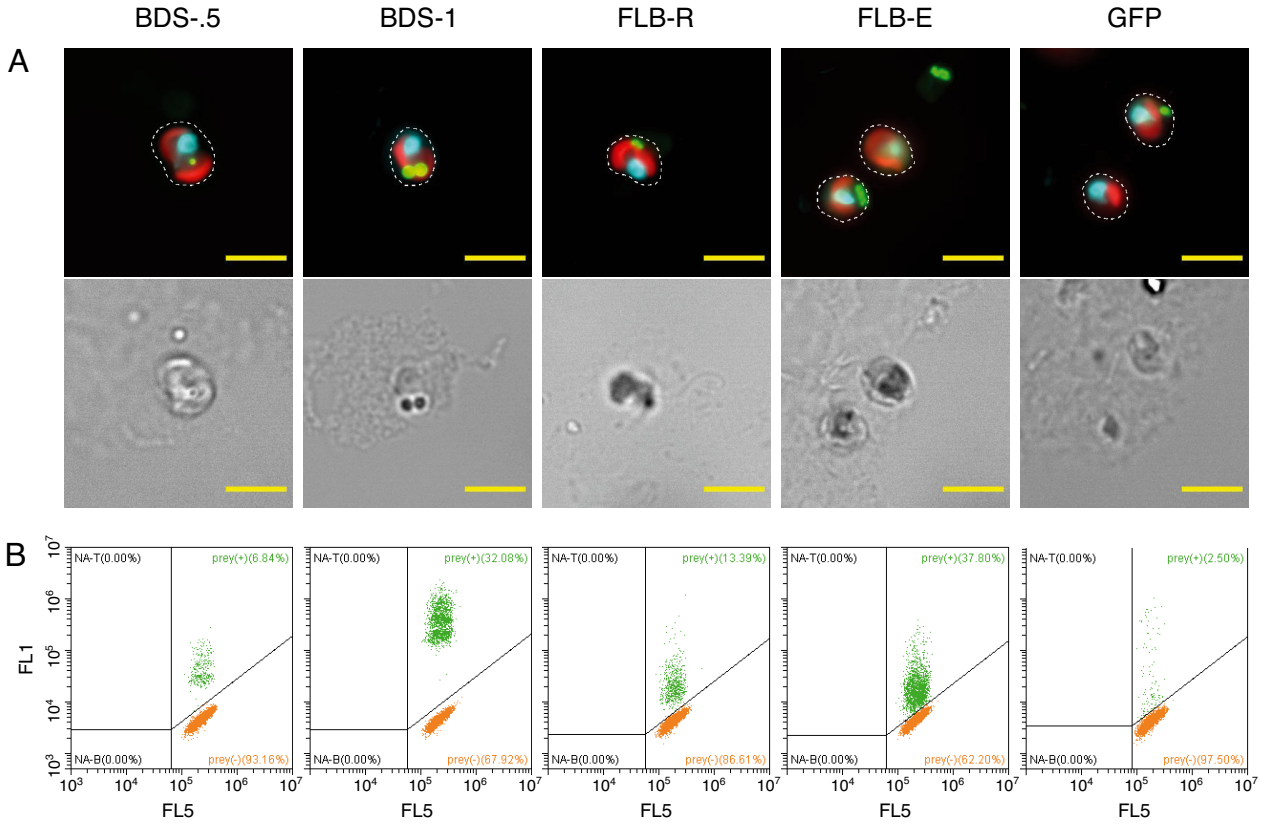

Fig. 1. (A) Images illustrating particle ingestion events for each prey type tested. Each image pair consists of a composite epifluorescence image of *Ochromonas triangulata* (top) and the corresponding brightfield image of the same cell (bottom). The epifluorescence images display the nucleus (cyan), chloroplasts (red) and surrogate prey (green). Cell contours are drawn from the brightfield image. All scale bars = 5 µm. (B) Flow cytometry scatter diagrams of food vacuole fluorescence (FL5) vs. prey fluorescence (FL1); green population: cells that ingested at least one fluorescently labelled tracer (FLT); orange population: actively feeding cells that did not ingest any FLTs. All scatter diagrams correspond to samples taken after 40 min incubation. See Table 1 for FLT type descriptions

vealed that actively feeding cells accounted for 99.3% (median value across all replicates) of total cells detected at the time of the experiment (Fig. S3). Across treatments, the higher fluorescence intensity of inert fluorescent beads made it easier to discriminate between prey-positive and prey-negative populations, although in all cases the separation was clear enough to permit visual discrimination along the FL1 channel in the FL5 vs. FL1 scatter diagrams (Fig. 1B).

Prey per cell observations for each replicate and timepoint increased linearly with incubation time up to 32 min after the addition of the fluorescent prey to the experimental flasks. Beyond this point, linearity began to deteriorate for the treatments showing higher values of *r*. This could indicate that tracer digestion or egestion by the feeding flagellate was starting to mask ingestion rates. For this reason, the last sampling point was excluded from further analysis.

Tracer ingestion rates differed for all treatments, both across prey types and across methodologies (Fig. 2, Table 2). Higher ingestion rates were associated with 2 of the 3 tracers belonging to the large size classes FLB-E and BDS-1. The former type showed the highest ingestion rates, consistently for both microscopy and flow cytometry. Relatively high rates were also consistently observed for the BDS-1 type, whereas all other treatments yielded at least 35% lower rates than these 2 tracers, suggesting a strong preference of *Ochromonas triangulata* for prey of large size. GFP-expressing *E. coli* cells were the only

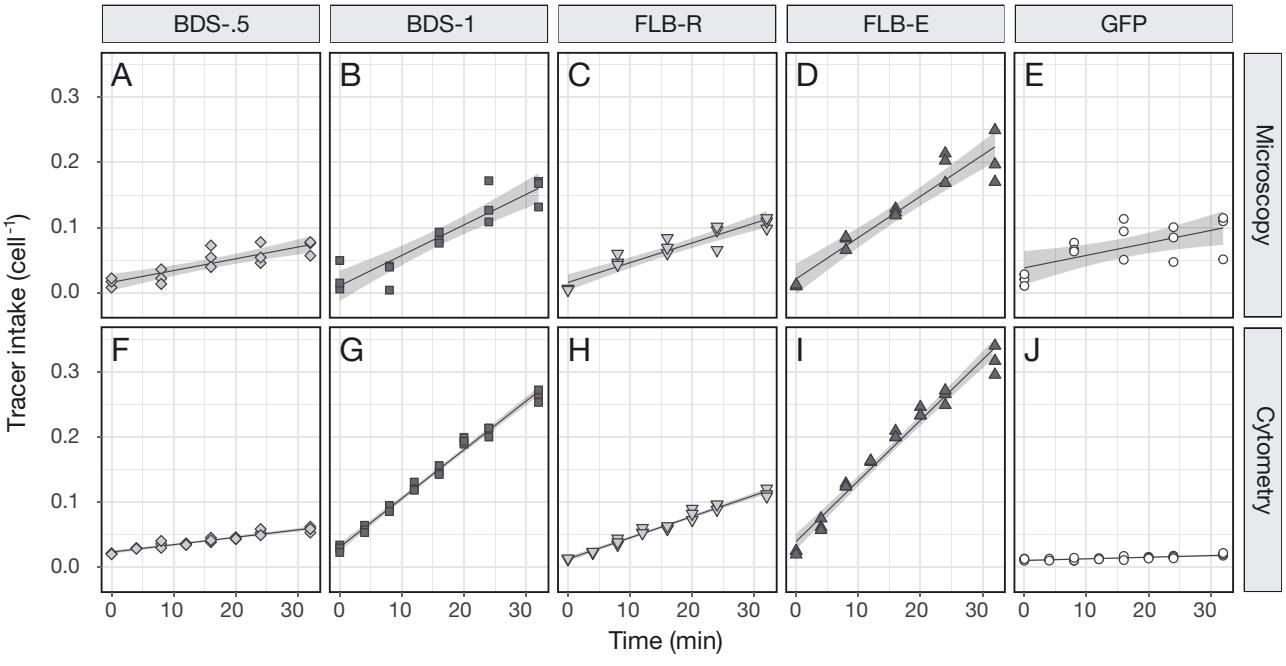

Fig. 2. Fluorescently labelled tracer (FLT) uptake by *Ochromonas triangulata* as measured with (A–E) epifluorescence microscopy or (F–J) flow cytometry. Each column corresponds to a different FLT type. Line: best linear fit to the data points; shaded area: uncertainty (SE) around the estimate. See Table 1 for FLT type descriptions

Table 2. Ingestion rate estimates and their associated standard error for each combination of methodology and fluorescently labelled tracer (FLT). See Table 1 for FLT type descriptions

FLT type	Density of inoculum ($\times 10^5$ ml^{-1})	Ingestion rate ($\times 10^{-3}$ min^{-1})		r^2		p	
		Cytometry	Microscopy	Cytometry	Microscopy	Cytometry	Microscopy
BDS-.5	1.460	1.14 ± 0.07	1.81 ± 0.30	0.9191	0.7372	<0.001	<0.001
BDS-1	1.415	7.48 ± 0.17	4.68 ± 0.54	0.9890	0.8505	<0.001	<0.001
FLB-R	1.480	3.26 ± 0.10	3.03 ± 0.30	0.9779	0.8903	<0.001	<0.001
FLB-E	1.553	9.31 ± 0.34	6.34 ± 0.55	0.9721	0.9106	<0.001	<0.001
GFP	1.570	0.25 ± 0.04	1.91 ± 0.61	0.6242	0.4319	<0.001	0.008

FLT that deviated from this pattern, belonging to the large size class but showing uptake rates similar to those observed for prey in the small size class. Unfortunately, almost no tracer ingestion could be detected via flow cytometry in the incubations with GFP-expressing *E. coli* cells. Since evidence of GFP-tagged prey uptake could be obtained under the microscope, we assume that this phenomenon must have been due to some experimental artefact associated with the live-cell flow cytometry assay. This may have involved a detrimental interaction between LS and GFP fluorescence or the GFP signal being quenched enzymatically over time in the food vacuoles. In any case, specific tests that attempt to unravel this effect were not performed and thus its mechanism remains unknown. As a consequence, data associated with the GFP-expressing prey treatment were excluded from further methodological comparison.

In comparing the 2 counting methodologies, the uncertainty associated with microscopy counting was clearly higher than that associated with the flow cytometry measurements. In all cases, the microscopy-based measurements led to higher standard errors of the regression compared to the corresponding estimates resulting from flow cytometry (Table 2). This difference ranged from 2- to 15-fold in magnitude. The smallest difference corresponded to the FLB-E prey type, which in turn yielded the highest uptake rates based on both methodologies. Relatively higher uncertainty in the flow cytometry estimate of the FLB-E treatment suggests that the fraction of unexplained variation increased proportionally with the value of the estimate, indicating that the model considered to score ingestion events via flow cytometry (see Section 2.7) worsens as ingestion rate increases. This is to be expected, since higher ingestion rates increase the probability of multiple ingestion events in individual cells, which are in turn neglected in the model. Nevertheless, the generally low tracer ingestion rates observed in this study (<0.1 min^{-1}; see Bratvold et al. 2000) ensure that the impact of this effect is minor. As a consequence of higher uncertainty associated with the microscopy estimates, the quality of the linear regression, evaluated by the regression coefficient r^2, was higher for cytometric counting when comparing each prey type across these 2 observational methods.

CRs were calculated from r following Eq. (1) (Fig. 3). As expected from the tracer uptake curves, each tracer–methodology combination yielded a unique estimate — with the exception of the FLB-R type, for which both estimates were in agreement.

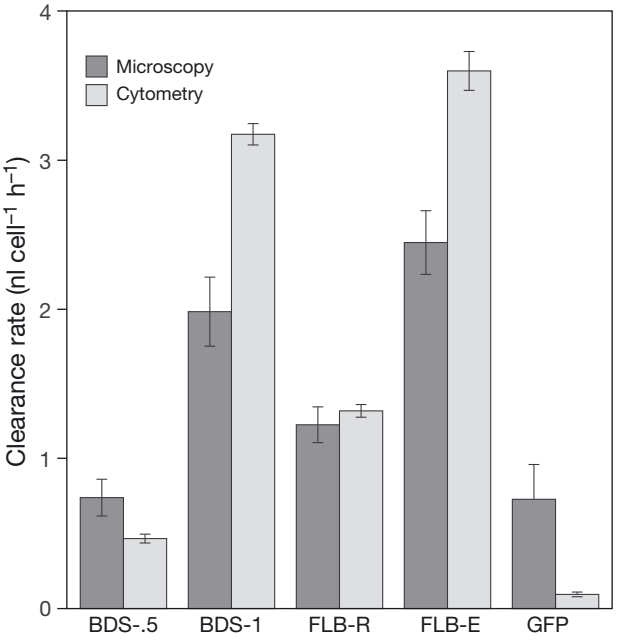

Fig. 3. Estimated clearance rates for each fluorescently labelled tracer (FLT) type. Error bars: SE associated with the estimate. See Table 1 for FLT type descriptions

However, both counting methodologies captured the same overall sequence in grazing rates across the prey types: BDS-.5 < FLB-R < BDS-1 < FLB-E. In this sequence, the highest CR estimates were from incubations with large prey size classes. Both BDS-1 and FLB-E treatments yielded rates between 2 and 3 nl $cell^{-1}$ min^{-1} based on microscopic counts and above 3 nl $cell^{-1}$ min^{-1} based on cytometric counts. In contrast, rates associated with the small size class remained below 1.4 nl $cell^{-1}$ min^{-1} irrespective of the counting approach.

Despite major overall differences in CRs spanning an 8-fold range, another pattern can be observed regardless of methodology: pairwise comparisons between small and large size classes within each methodology featured a greater difference than comparisons among prey quality classes (i.e. inert vs. dead) of the same size class. Hence, CRs for both incubations with either differentially sized beads or FLB differed >6- or ~3-fold, respectively, whereas differences between quality classes within each size class (i.e. BDS-.5 vs. FLB-R; BDS-1 vs. FLB-E) were all lower than 2-fold (with the exception of BDS-.5 to FLB-R for the cytometry estimate, which was 2.8 times higher for the FLB type). Based on these observations, we conclude that tracer size is a stronger driver than particle quality in defining the magnitude of CR estimates. However, the living prey type constituted an exception to this pattern. Despite

being a comparatively large size, rates associated with this treatment fell within the range associated with the small size class. When compared to the other types within the large class, rates differed by a factor of 2.7 for BDS-1 and 3.3 for FLB-E. These represented the largest differences in magnitude within types of the same size class.

When comparing observational methodologies for each prey type, the differences in observed ingestion or CRs appear to be relatively minor. With the exception of the FLB-R treatment, in which there was no significant difference, a difference of ~1.5 was consistently observed for the other 3 treatments. Only the directionality differed: while the microscopy-based estimates reported a higher grazing rate for the BDS-.5 type, the opposite was seen for the BDS-1 and FLB-E types. Thus, the choice of methodology (microscopy vs. cytometry) appears to have less of an impact on grazing rate estimates even though processivity and automation of flow cytometry hold potential for higher analytical precision and analyses of larger sample sets.

4. DISCUSSION

In general terms, our CR estimates are in accordance with values reported in the literature for other *Ochromonas* strains (Chrzanowski & Šimek 1990, Boenigk et al. 2004). Nonetheless, our results suggest that the differences in grazing estimates associated with prey size are larger than those associated with either prey quality or observational methodology when using short-term tracer incubation experiments to measure bacterivory.

Indeed, prey size has previously been recognized as an influential factor in the grazing behavior of phagotrophic flagellates, both in culture and in natural samples (Andersson et al. 1986, Chrzanowski & Šimek 1990, Gonzalez et al. 1990, Jürgens & Matz 2002, Schmidtke et al. 2006), and therefore it is expected to be a potentially strong skewing factor on FLT-based bacterivory estimates. To mitigate this effect, FLB prepared from amended natural communities could be used to measure uptake rates (as initially suggested by Sherr & Sherr 1993) since such FLBs would convey a wide representation of size and shapes, in principle resembling those present in the natural assemblages. However, this is a labor-intensive approach and restricts, by design, each FLB preparation to its environment of origin. A further complication is the challenge that would arise when comparing results between different studies in the absence of standardized prey. The most practical solution would be to synchronously use multiple-sized fluorescent microspheres (Jürgens & Güde 1994), but CRs would ultimately depend on the ratios between size classes (as seen e.g. in Chrzanowski & Šimek 1990 for FLB). Reporting a range of potential grazing rates based on estimates spanning a collection of FLTs differing in size could be another solution — either in parallel incubations or simultaneously — if, for instance, the different FLTs also differ in their fluorescent properties. Nonetheless, grazing rates estimated from FLT uptake experiments will inevitably be sensitive to the size of tracers employed.

Tracer quality can also potentially compromise bacterivory estimates. In our experiment, differences in prey quality, when comparing among FLTs of the same size class, resulted in the smallest differences among estimated rates in almost all cases, with the exception of the GFP-tagged living cells. Tracer quality has previously been suggested to be a confounding element when estimating bacterivory based on FLT incubations, particularly when living fluorescent prey is compared to heat-killed, 5-DTAF-stained bacteria (Fu et al. 2003, Bochdansky & Clouse 2015). In these earlier studies, grazing rates of model flagellates in culture were estimated from either FLB- or GFP-expressing prey surrogates of comparable sizes; Fu et al. (2003) reported higher grazing rates with living prey whereas Bochdansky & Clouse (2015) reported the opposite. Regardless of the directionality, both studies showed differences of a factor of ~1.5 among types, which accounts for approximately half the difference reported here. This difference could be related to the nature of the model predator (*Paraphysomonas imperforata* was used by Fu et al. 2003, whereas *Neobodo saltans* and *Cafeteria roenbergensis* were chosen by Bochdansky & Clouse 2015), which adds up to variation brought about by tracer size (Fu et al. 2003 used a tracer comparable to the large size class described here, whereas Bochdansky & Clouse 2015 used prey of a smaller size). Differences could also be related to observational methodology (Fu et al. 2003 employed flow cytometry, whereas Bochdansky & Clouse 2015 relied on microscopy). In any case, all these results combined point towards higher complexity in prey selection by the predator than just preference based on size.

Finally, the observational methodology of choice influences both the quality and magnitude of the grazing estimate. In the present study, flow cytometry-based estimates rely on a simple assumption: one prey-positive event corresponds to a single ingestion

event. Other strategies have been previously proposed, such as modelling uptake based on a Poisson distribution (González 1999), truncated Poisson distribution (Bratvold et al. 2000) or monitoring FLB depletion over longer time periods (Fu et al. 2003). However, Poisson-based approaches are not adequate to describe the low uptake rates observed in our experiment, and the post hoc application of the latter is not appropriate for our study design because of the short incubation times. Admittedly, our methodological approach neglects cases of multiple ingestion by a single predator cell and thus will result in underestimates of grazing rates. However, the probability of multiple ingestion events is small when low values of r are observed (<0.1 cell^{-1} min^{-1}; see Bratvold et al. 2000). This is the case in our study (0.14 median frequency of multiple ingestion events based on microscopy observations with no relationship with time; Fig. S5), and therefore we believe that the extent of the underestimation is low and our assumption remains appropriate for the analysis presented here.

Flow cytometry delivered greater precision in estimates of grazing rates compared to the customary strategy based on epifluorescence microscopy. This is clear from our results and is in agreement with a recently published study (Costa et al. 2022) in which the authors found significant differences in ingestion rates associated with nutrient treatments that could not be significantly resolved based on epifluorescence microscopy. Even so, differences in the magnitude of the estimates produced by either methodology are not striking, and therefore we feel that microscopy is still a valid option when practical or logistic limitations prevent the use of flow cytometry. In addition, epifluorescence microscopy can provide additional layers of information for the expert examiner through visual confirmation of ingestion events and morphological identification of the predators. Indeed, flow cytometry has been shown to be sensitive to confounding artefacts that could otherwise be visually recognized, such as FLT–flagellate associations due to flagellate senescence (Wilken et al. 2019). Food vacuole staining, although not devoid of specificity issues (Rose et al. 2004, Wilken et al. 2019, but see Carvalho & Granéli 2006), can contribute to minimizing the impact of such circumstances when used in conjunction with FLT uptake, as done in our experiment. In the case of predator identification, flow cytometry still enables a similar output since the sample can potentially be fractionated into cytometric groups based on multicolor gating by taking advantage of natural pigmentation or complementing the experiment with additional staining strategies, such as staining of food vacuoles or other organelles. However, the availability of fluorophores that target functional features on the predators is still limited, and microscopic identification of phagotrophic eukaryotes, despite requiring extensive experience, is currently more developed than characterization based on flow cytometry.

High sample complexity might result in additional challenges when delineating prey-positive and prey-negative populations in the flow cytometer, but it can equally well be a strong uncertainty factor when examining a sample under the microscope. When sample complexity is high, the quality of the output with either methodology will still depend on the skill and expertise of the investigator. On the other side of the same spectrum, low predator density in the sample can also pose a severe limitation in flow cytometry. Despite its capacity to screen large numbers of cells in a single run, the running volumes on a flow cytometer are still restricted to the ml level. Screening substantial volumes of a sample might be needed when predator densities are low, and total grazing pressure on bacteria might be underestimated when low sample volumes are considered. For instance, the density of a highly active bacterivorous ciliate population in a lake can approximate 50 cells ml^{-1} (Lischke et al. 2016); running a flow cytometer at 75 µl min^{-1} (as done here) would imply the observation of only ~20 cells in >5 min running time. This would inevitably compromise both the precision and the validity of the estimate due to low sample size and long analysis time, respectively. As a result, any environment where predator abundance is low would present a challenge to flow cytometry.

Despite these potential limitations, there is still a broad range of conditions in which flow cytometry could be a promising tool to estimate bacterivory rates with improved precision. Undoubtedly, flow cytometry analysis times are much shorter than those necessary for microscopy observation, allowing the screening of orders of magnitude larger populations and/or a larger number of samples. Moreover, if flow cytometry is employed for the analysis of living samples (i.e. non-fixed), all potential biases associated with fixation (such as particle egestion; Caron 2001) and slide preparation are avoided, yielding more realistic estimates of bacterivory. If analysis of live samples is not practically possible, fixed samples are still suitable for flow cytometry and can be used both for predator-associated prey fluorescence and estimates of community-level grazing rates from FLT removal. To the best of our knowledge, to date there

has only been one study where flow cytometry and short-term FLT incubations have been used to estimate bacterial grazing rates to inform about ecological processes (Costa et al. 2022). We believe that possibilities exist for more refined grazing rate estimates based on flow cytometry, by developing strategies to target group-specific grazing rates when cytometric groups are identified or establishing multicolor gating routines to systematically bypass sample complexity. Thus, we argue that flow cytometry is a robust, precise and practical methodology to be considered when precise grazing rates need to be estimated.

Acknowledgements. The authors thank Ian Probert (Roscoff Culture Collection) and Maliheh Mehrshad and Prune Leroy (Swedish University of Agricultural Sciences) for providing the strains used in this study. J.F. also thanks Ingrid Bergman for invaluable assistance during the experimental procedures. This work was financed through the Marie Skłodowska-Curie ITN project SINGEK (grant agreement no. H2020-MSCA-ITN-2015-675752). The contribution of 3 anonymous reviewers was fundamental in improving the quality of the original manuscript.

LITERATURE CITED

Anderson R, Jürgens K, Hansen PJ (2017) Mixotrophic phytoflagellate bacterivory field measurements strongly biased by standard approaches: a case study. Front Microbiol 8:1398

Andersson A, Larsson U, Hagström Å (1986) Size-selective grazing by a microflagellate on pelagic bacteria. Mar Ecol Prog Ser 33:51–57

Arenovski AL, Lim EL, Caron DA (1995) Mixotrophic nanoplankton in oligotrophic surface waters of the Sargasso Sea may employ phagotrophy to obtain major nutrients. J Plankton Res 17:801–820

Azam F, Fenchel T, Field JG, Gray JS, Meyer-Reil LA, Thingstad F (1983) The ecological role of water-column microbes in the sea. Mar Ecol Prog Ser 10:257–263

Berges JA, Franklin DJ, Harrison PJ (2001) Evolution of an artificial seawater medium: improvements in enriched seawater, artificial water over the last two decades. J Phycol 37:1138–1145

Bird DF, Kalff J (1987) Algal phagotrophy: regulating factors and importance relative to photosynthesis in *Dinobryon* (Chrysophyceae). Limnol Oceanogr 32:277–284

Bochdansky AB, Clouse MA (2015) New tracer to estimate community predation rates of phagotrophic protists. Mar Ecol Prog Ser 524:55–69

Boenigk J, Stadler P, Wiedlroither A, Hahn MW (2004) Strain-specific differences in the grazing sensitivities of closely related ultramicrobacteria affiliated with the *Polynucleobacter* cluster. Appl Environ Microbiol 70: 5787–5793

Bratvold D, Srienc F, Taub SR (2000) Analysis of the distribution of ingested bacteria in nanoflagellates and estimation of grazing rates with flow cytometry. Aquat Microb Ecol 21:1–12

Caron DA (2001) Protistan herbivory and bacterivory. Methods Microbiol 30:289–315

Carvalho WF, Granéli E (2006) Acidotropic probes and flow cytometry: a powerful combination for detecting phagotrophy in mixotrophic and heterotrophic protists. Aquat Microb Ecol 44:85–96

Chrzanowski TH, Foster BLL (2014) Prey element stoichiometry controls ecological fitness of the flagellate *Ochromonas danica*. Aquat Microb Ecol 71:257–269

Chrzanowski TH, Šimek K (1990) Prey-size selection by freshwater flagellated protozoa. Limnol Oceanogr 35: 1429–1436

Cleven EJ, Weisse T (2001) Seasonal succession and taxon-specific bacterial grazing rates of heterotrophic nanoflagellates in Lake Constance. Aquat Microb Ecol 23: 147–161

Costa MRA, Sarmento H, Becker V, Bagatini IL, Unrein F (2022) Phytoplankton phagotrophy across nutrients and light gradients using different measurement techniques. J Plankton Res 44:508–521

Domaizon I, Viboud S, Fontvieille D (2003) Taxon-specific and seasonal variations in flagellates grazing on heterotrophic bacteria in the oligotrophic Lake Annecy—importance of mixotrophy. FEMS Microbiol Ecol 46: 317–329

Fu Y, O'Kelly C, Sieracki M, Distel DL (2003) Protistan grazing analysis by flow cytometry using prey labeled by *in vivo* expression of fluorescent proteins. Appl Environ Microbiol 69:6848–6855

González JM (1999) Bacterivory rate estimates and fraction of active bacterivores in natural protist assemblages from aquatic systems. Appl Environ Microbiol 65:1463–1469

Gonzalez JM, Sherr EB, Sherr BF (1990) Size-selective grazing on bacteria by natural assemblages of estuarine flagellates and ciliates. Appl Environ Microbiol 56: 583–589

Grujčić V, Kasalický V, Šimek K (2015) Prey-specific growth responses of freshwater flagellate communities induced by morphologically distinct bacteria from the genus *Limnohabitans*. Appl Environ Microbiol 81:4993–5002

Hahn MW, Stadler P, Wu QL, Pöckl M (2004) The filtration–acclimatization method for isolation of an important fraction of the not readily cultivable bacteria. J Microbiol Methods 57:379–390

Hewes CD, Holm-Hansen O (1983) A method for recovering nanoplankton from filters for identification with the microscope: the filter–transfer–freeze (FTF) technique. Limnol Oceanogr 28:389–394

Jürgens K, Güde H (1994) The potential importance of grazing-resistant bacteria in planktonic systems. Mar Ecol Prog Ser 112:169–188

Jürgens K, Matz C (2002) Predation as a shaping force for the phenotypic and genotypic composition of planktonic bacteria. Ant Leeuwenhoek 81:413–434

Kasalický V, Jezbera J, Hahn MW, Šimek K (2013) The diversity of the *Limnohabitans* genus, an important group of freshwater bacterioplankton, by characterization of 35 isolated strains. PLOS ONE 8:e58209

Keller MD, Selvin RC, Claus W, Guillard RRL (1987) Media for the culture of oceanic ultraphytoplankton. J Phycol 23:633–638

Keller MD, Shapiro LP, Haugen EM, Cucci TL, Sherr EB, Sherr BF (1994) Phagotrophy of fluorescently labeled bacteria by an oceanic phytoplankter. Microb Ecol 28: 39–52

Lischke B, Weithoff G, Wickham SA, Attermeyer K and others (2016) Large biomass of small feeders: ciliates may dominate herbivory in eutrophic lakes. J Plankton Res 38:2–15

Massana R, Unrein F, Rodríguez-Martínez R, Forn I, Lefort T, Pinhassi J, Not F (2009) Grazing rates and functional diversity of uncultured heterotrophic flagellates. ISME J 3:588–596

Pålsson C, Granéli W (2003) Diurnal and seasonal variations in grazing by bacterivorous mixotrophs in an oligotrophic clearwater lake. Arch Hydrobiol 157: 289–307

Princiotta SDV, Sanders RW (2017) Heterotrophic and mixotrophic nanoflagellates in a mesotrophic lake: abundance and grazing impacts across season and depth. Limnol Oceanogr 62:632–644

Rose JM, Caron DA, Sieracki ME, Poulton N (2004) Counting heterotrophic nanoplanktonic protists in cultures and aquatic communities by flow cytometry. Aquat Microb Ecol 34:263–277

Sanders RW, Porter KG, Bennett SJ, DeBiase AE (1989) Seasonal patterns of bacterivory by flagellates, ciliates, rotifers, and cladocerans in a freshwater planktonic community. Limnol Oceanogr 34:673–687

Schmidtke A, Bell EM, Weithoff G (2006) Potential grazing impact of the mixotrophic flagellate *Ochromonas* sp. (Chrysophyceae) on bacteria in an extremely acidic lake. J Plankton Res 28:991–1001

Sherr EB, Sherr BF (1993) Protistan grazing rates via uptake of fluorescently labelled prey. In: Kemp PF, Sherr EB, Sherr BF, Cole JJ (eds) Handbook of methods in aquatic microbial ecology, 1st edn. Lewis Publishers, Boca Raton, FL, p 695–702

Šimek K, Nedoma J, Pernthaler J, Posch T, Dolan JR (2002) Altering the balance between bacterial production and protistan bacterivory triggers shifts in freshwater bacterial community composition. Ant Leeuwenhoek 81: 453–463

Šimek K, Nedoma J, Znachor P, Kasalický V, Jezbera J, Horňák K, Sed'a J (2014) A finely tuned symphony of factors modulates the microbial food web of a freshwater reservoir in spring. Limnol Oceanogr 59:1477–1492

Vazquez-Dominguez E, Peters F, Gasol JM, Vaqué D (1999) Measuring the grazing losses of picoplankton: methodological improvements in the use of fluorescently labeled tracers combined with flow cytometry. Aquat Microb Ecol 20:119–128

Wilken S, Soares M, Urrutia-Cordero P, Ratcovich J, Ekvall MK, Van Donk E, Hansson LA (2018) Primary producers or consumers? Increasing phytoplankton bacterivory along a gradient of lake warming and browning. Limnol Oceanogr 63:S142–S155

Wilken S, Yung CCM, Hamilton M, Hoadley K and others (2019) The need to account for cell biology in characterizing predatory mixotrophs in aquatic environments. Philos Trans R Soc B 374:20190090

Editorial responsibility: Josep Gasol, Barcelona, Spain
Reviewed by: 3 anonymous referees

Submitted: July 8, 2022
Accepted: February 15, 2023
Proofs received from author(s): March 20, 2023